

# Super Enhancer-driven LncRNA UNC5B-AS1 Inhibits Inflammatory Phenotypic Transition in Smooth Muscle Cells via Lactylation Modification

Xiangrui Zhu<sup>1</sup>, Xiangming Pang<sup>1</sup>, Xiaoying Wang<sup>2</sup>, Xiaoyu Guan<sup>5</sup>, Zhaosi Wang<sup>1</sup>, Lixin Zhang<sup>1,3</sup>, Xiaodong Zheng<sup>3</sup>, Fei Li<sup>4</sup>, Jian Mei<sup>1</sup>, Langlin Ou<sup>1</sup>, Yuxiang Liu<sup>1</sup>, Zitong Meng<sup>1</sup>, Yingli Chen<sup>1</sup>, Cui Ma<sup>1,3\*</sup>

<sup>1</sup> College of Medical Laboratory Science and Technology, Harbin Medical University (Daqing), Daqing 163319, P. R. China.

<sup>2</sup> College of Pharmacy, Harbin Medical University (Daqing), Daqing 163319, P. R. China.

<sup>3</sup> Central Laboratory of Harbin Medical University (Daqing), Daqing 163319, P. R. China.

<sup>4</sup> College of Basic Medicine, Harbin Medical University (Daqing), Daqing 163319, P. R. China.

<sup>5</sup> College of Pharmacy, Harbin Medical University, Harbin 150081, P.R. China.

**Short title:** UNC5B-AS1: A Target for Inflammation in PSMCs

\*Corresponding author: Cui Ma, Email: macui0804@sina.com, Central Laboratory of Harbin Medical University (Daqing), Daqing 163319, P. R. China.

**Total word count:7401**

# Abstract

**Background:** The phenotypic transition of pulmonary artery smooth muscle cells (PASMCs) is a central pathological alteration in pulmonary artery remodeling that contributes to pulmonary hypertension (PH). The specific role of long noncoding RNAs (lncRNAs), especially super enhancer (SE)-driven lncRNAs, in the phenotypic transformation of PASMCs induced by hypoxia remains unclear. The objective of this study is to determine the mechanistic role of the super enhancer-driven lncRNA UNC5B-AS1 in phenotypic transformation of PASMCs and hypoxia-induced vascular remodeling.

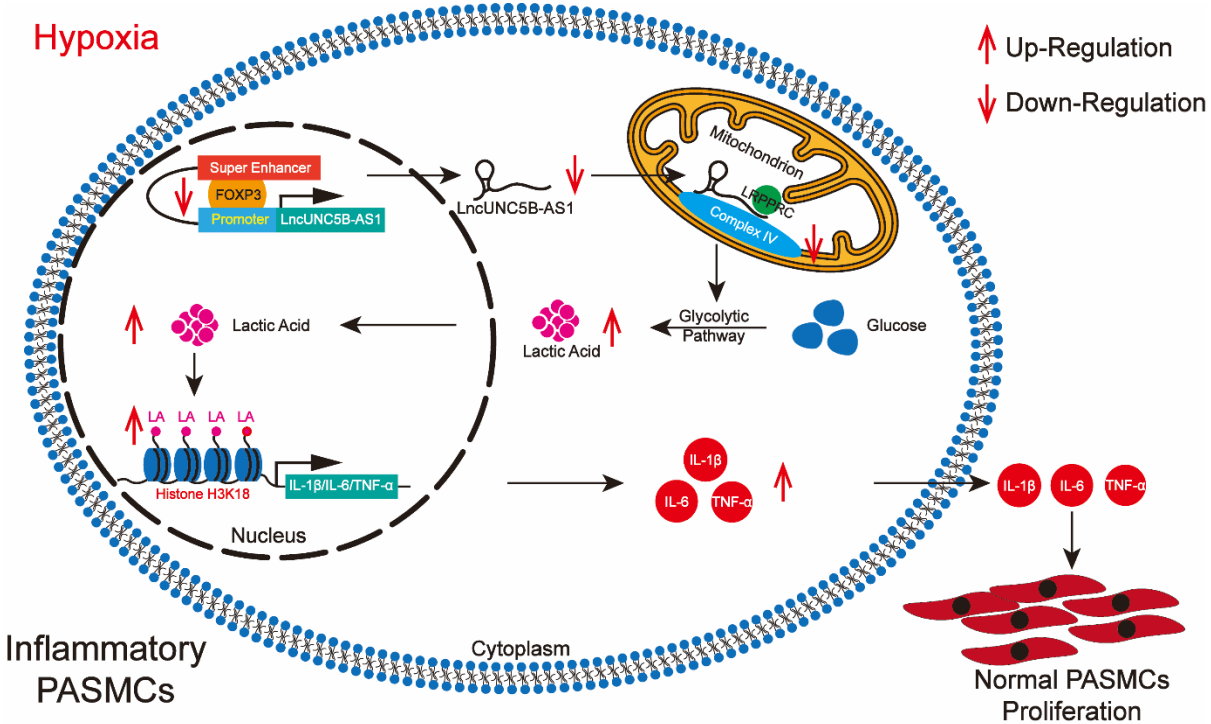
**Methods:** The lncRNA UNC5B-AS1 regulated by super-enhancers was identified in hypoxic human PASMCs through RNA sequencing and H3K27ac ChIP sequencing. Overexpression of lncRNA UNC5B-AS1 in human PASMCs was performed to elucidate its role in the pathogenesis of PH. A conserved functional fragment of lncRNA UNC5B-AS1 was used for the treatment of mouse PH.

**Results:** In PASMCs, we have identified a SE-driven lncRNA called UNC5B-AS1 that regulates phenotype transition. It is transcriptionally activated by the transcription factor FOXP3. We demonstrate that UNC5B-AS1, as a molecular scaffold in mitochondria, stabilizes the interaction between LRPPRC, which is rich in leucine, and oxidative respiratory chain complex IV. This complex regulates the lactylation modification level of upstream promoter regions of inflammatory genes IL-1 $\beta$ , IL-6, and TNF- $\alpha$  by influencing the glycolytic pathway in PASMCs under hypoxic conditions, ultimately affecting the inflammatory phenotype transition of PASMCs.

**Conclusions:** Our findings identify the SE-driven lncRNA UNC5B-AS1 as a novel regulatory

factor in hypoxia-induced phenotypic switch of PASMCs, and suggest that overexpression of UNC5B-AS1 may represent a promising therapeutic strategy for PH.

**Key Words:** Super Enhancer; Long noncoding RNA; Smooth Muscle Cells; Inflammatory Phenotypic; Pulmonary Hypertension; Lactylation Modification



Non-standard Abbreviations and Acronyms

UNC5B-AS1	UNC5B antisense RNA 1
PASMCs	Pulmonary Artery Smooth Muscle Cells
PH	Pulmonary Hypertension
lncRNA	Long Noncoding RNA
SE	Super Enhancer
ChIP	Chromatin Immunoprecipitation
LRPPRC	Leucine-Rich PPR Motif-Containing Protein
FOXP3	Forkhead Box Protein P3

IL	Interleukin
TNF- $\alpha$	Tumor Necrosis Factor Alpha
OPN	Osteopontin
KLF4	Krüppel-Like Factor 4
CNN1	Calponin-1
SM22 $\alpha$	Smooth Muscle Protein 22-alpha
HKII	Hexokinase II
PKM2	Pyruvate Kinase M2
ECAR	Extracellular Acidification Rate
CM	Conditioned Medium
SuHx	Sugen5416/Hypoxia
AAV5	5 Adenovirus-Associated Virus
H&E	Hematoxylin And Eosin Staining
UA1CF	UNC5B-AS1 Conserved Fragment
RV/LV	Right Ventricle/Left Ventricle
RVSP	Right Ventricular Systolic Pressure
PAAT	Pulmonary Artery Acceleration Time
PAVTI	Pulmonary Artery Velocity-Time Integral
EF	Ejection Fraction

## Introduction

The pathology of pulmonary hypertension (PH) is complex and associated with cardiac, pulmonary, and systemic diseases that contribute to morbidity and mortality<sup>1</sup>. PH is

characterized by inflammation, pulmonary vascular remodeling, and pulmonary vascular embolism leading to elevated pulmonary arterial pressure and resistance, right ventricular dysfunction, left ventricular compression, and subsequent heart failure<sup>2,3</sup>. The remodeling process occurs throughout the pulmonary arterial vasculature and involves medial thickening, which is driven by increased proliferation and hypertrophy of pulmonary artery smooth muscle cells (PASMCs), its principal cellular component<sup>4</sup>. However, there is heterogeneity among PASMCs, which can exhibit markedly different changes in proliferative, inflammatory, and extracellular matrix production during remodeling<sup>5-7</sup>. Typically, PASMCs express high levels of contractile proteins such as  $\alpha$ -smooth muscle actin ( $\alpha$ -SMA), calponin, SM22 $\alpha$  and other differentiation markers, which is accompanied by a low rate of proliferation<sup>5,8,9</sup>. Under pathological conditions, PASMCs acquire inflammatory cell markers and release inflammatory cytokines, such as interleukin (IL)-1 $\beta$ , IL-6 and tumor necrosis factor (TNF)- $\alpha$ , contributing to the proinflammatory environment, which is followed by vessel injury and remodeling<sup>10</sup>. These findings suggest that the inflammatory phenotypic transition of PASMCs can contribute to the development of PH.

Long noncoding RNAs (lncRNAs) are non-protein-coding transcripts with lengths greater than 200 nucleotides<sup>11</sup>. An increasing number of studies have shown that lncRNAs play important roles in diverse cellular processes, including proliferation<sup>12</sup>, apoptosis<sup>13</sup>, migration<sup>14</sup>, invasion<sup>15</sup>, chromatin remodeling<sup>16</sup>, metabolism<sup>17</sup>, and immune escape<sup>18</sup>. Super enhancers (SEs) are a widespread class of chromatin regulatory elements in the genome that are closely associated with the expression levels of specific genes<sup>19</sup>. lncRNAs driven by SEs are lncRNAs expressed near SEs that regulate gene expression through interactions with SEs. In gliomas,

the SE-driven lncRNA TMEM44-AS1 promotes tumor cell growth through the formation of a positive feedback loop with MYC<sup>20</sup>. The lncRNA NEAT1 has been identified as an SE-driven lncRNA that controls the lineage fate of bone marrow mesenchymal stem cells (BMSCs) during skeletal aging by affecting mitochondrial function<sup>21</sup>. Moreover, lncRNA CARMN has been confirmed to be driven by an SE in vascular smooth muscle cells and is involved in maintaining the contractile phenotype of smooth muscle cells<sup>22</sup>. However, the mechanism of SE-driven lncRNAs in PSMCs inflammatory phenotypic transition and PH development needs to be further examined.

Emerging evidence shows that lactate has regulatory functions in physiologic and pathologic cells and induces dramatic changes in gene expression, suggesting that lactate is not simply a waste product of glycolysis<sup>23</sup>. In response to hypoxia, cells undergo metabolic reprogramming by inhibiting oxidative phosphorylation and enhancing glycolysis, thereby stimulating the production of lactate<sup>24</sup>. Recent studies indicated that hypoxia induced intracellular lactate production and increased histone K1a but not K4c levels in MCF-7 cells<sup>23</sup>. Lactate-derived lactylation of histone lysine residues is an epigenetic modification that directly stimulates gene transcription<sup>25</sup>. Histone lactylation modification can influence the transition of inflammatory macrophage phenotypes, thereby impacting inflammation levels and participating in the progression of related diseases<sup>25,26</sup>. Thus, controlling the glycolytic switch via lactylation suggests novel therapeutic opportunities to treat PH.

In this study, we showed for the first time that lncRNA UNC5B antisense RNA 1(UNC5B-AS1, Chr10q22.1) was regulated by SEs in PSMCs. It is transcriptionally activated by the transcription factor forkhead box protein P3 (FOXP3). Our data indicated that UNC5B-AS1

served as a molecular scaffold in mitochondria and interacted with leucine-rich PPR motif-containing protein (LRPPRC) and mitochondrial complex IV. Under hypoxic conditions, the loss of UNC5B-AS1 expression impaired mitochondrial oxidative phosphorylation, leading to abnormal activation of glycolysis. The accumulation of lactate due to the activation of glycolysis in hypoxia, affected the lactylation of inflammatory factor promoters in PSMCs and ultimately promoted the transition of PSMCs to an inflammatory phenotype and contributed to the progression of PH.

## **Methods**

### **Animal**

This study used adult male C57BL/6 mice (6-9 weeks old) obtained from the Experimental Animal Center of the Second Affiliated Hospital of Harbin Medical University. All experimental procedures have obtained approval from the Ethics Committee of Harbin Medical University (HMUDQ20230831001). All animal studies were conducted in compliance with the National Institutes of Health (NIH) guidelines for the care and use of laboratory animals. The RNA cloning constructs, and serotype 5 adenovirus-associated virus (AAV5) were synthesized by GeneChem (China). After randomization, the mice were divided into groups and intranasally infected with  $10^{11}$  genome equivalents of AAV5 vector solution diluted with 20  $\mu$ L of Hank's balanced salt after isoflurane anesthesia. After 14 days, the mice were assigned to normoxia (21% O<sub>2</sub>) and hypoxia (10% O<sub>2</sub>) conditions, as described in previous studies<sup>27</sup>. In the Sugen hypoxia model, the mice were injected once per week with the VEGF inhibitor SU5416 (Med Chem Express, USA) at a concentration of 20 mg/kg. Subsequently, the mice were subjected to 3 weeks of hypoxia (10% O<sub>2</sub>) followed by 2 weeks of reoxygenation (21%

O<sub>2</sub>). The control group was maintained in a normal oxygen environment, and the oxygen concentration was continuously monitored for 5 weeks using an oxygen analyzer (BioSpherix, USA). After constructing the model, euthanasia was performed on mice using a small animal euthanasia system (Yuyan Instruments, China) by inhalation of 100% CO<sub>2</sub>, followed by cervical dislocation as a secondary confirmation of death. Lung tissue was collected for further experiments. The right ventricular (RV) hypertrophy index (RV/(LV+S)), is calculated by dividing the weight of the right ventricular free wall by the sum of the weight of the septum plus the left ventricular free wall.

### **Small Animal Echocardiography and Right Ventricular Systolic Pressure**

After the completion of hypoxia and SU5416 treatment, the mice underwent echocardiography using the Vevo2100 imaging system equipped with an 18 to 38MHz transducer probe (VisualSonics, Canada), as described previously<sup>28</sup>. Mice were anesthetized using a desktop anesthesia machine (Harvard Apparatus, USA) with inhalation of a concentration of 1% to 3% isoflurane. The mice were placed on a preheated imaging platform and the respiratory rate was continuously monitored throughout the entire echocardiography process. The pulmonary artery acceleration time (PAAT) and pulmonary artery velocity-time integral (PAVTI) were measured using pulse wave Doppler. Transthoracic echocardiography was performed in the short-axis view at the level of the sternum to measure left ventricular ejection fraction at end-diastole and end-systole. All measurements were performed by experienced researchers, and data analysis was conducted in a blinded manner using Vevo2100 software. Right ventricular systolic pressure was measured using the PowerLab monitoring system (AD Instruments, USA). The pressure catheter (Scisense Inc) was inserted into the right



ventricular vein via the superior vena cava, and right ventricular systolic pressure was continuously recorded for 10 to 30 minutes.

### **ChIP-seq**

ChIP-seq was performed by Guangzhou Epibiotek Co., Ltd. Briefly, the cells were cross-linked with 1% formaldehyde for 10 minutes, followed by quenching the cross-linking reaction with 0.125M glycine. The cells were then frozen on dry ice and stored until further use. After isolating the cell nuclei, the chromatin was sheared to fragment it into sizes ranging from 200 to 500 bp. 5 µg of anti-H3K27ac antibody (Cell Signaling) was incubated overnight with the fragmented chromatin. Protein A magnetic beads were used to capture immune complexes. The chromatin was eluted in reverse cross-linking buffer followed by incubate the tube at 65°C for 3h. After digestion with RNase and Proteinase K, the fragments were purified and quantified. ChIP DNA was processed for library generation using the QIAseq Ultralow Input Library Kit (QIAGEN) following the manufacturer's protocol. After library construction, the samples were subjected to sequencing analysis.

### **RNA-seq**

PASMCs cultured under normoxia/hypoxia conditions were harvest or RNA-seq. Total RNA was isolated using TRIzol reagent (Thermo Fisher Scientific, Massachusetts) according to the manufacturer's protocol. VAHTS Stranded mRNA-seq Library Prep Kit for Illumina V2 (Vazyme Biotech, NR612-02) was used for library preparation according to the instructions. The libraries were then sequenced on the Illumina NovaSeq 6000 platform by Epibiotek Co., Ltd. in Guangzhou.

### **Statistical Analysis**

The statistical analysis was performed using GraphPad Prism 8 software. Prior to statistical testing, the data were checked for normality and homogeneity of variances (F test). Student's t-test (unpaired) was used for analyzing data with equal variances in two groups, while Welch's corrected t-test was used for analyzing data with unequal variances in two groups. One-way analysis of variance (ANOVA) with Tukey's post hoc test was used to compare multiple groups with equal variances, while Brown-Forsythe and Welch's ANOVA with Tamhane T2 post hoc test were used to compare multiple groups with unequal variances. Nonparametric analysis was used for non-normally distributed data, including Mann-Whitney U test or Kruskal-Wallis test for two group analysis, followed by Dunn's post hoc test for >2 groups. Data are presented as mean  $\pm$  SEM, and a P value of <0.05 is considered statistically significant.

## Results

### **UNC5B-AS1 is a super enhancer-driven lncRNA that is downregulated by hypoxia.**

To identify differentially expressed lncRNAs in PH, we performed RNA-seq and H3K27ac ChIP-seq assays on PSMCs subjected to normoxia/hypoxia. Our results revealed significant downregulation of UNC5B-AS1 under hypoxic conditions (Fig.1A, B). H3K27ac ChIP-seq analysis was used to identify super enhancers in the upstream regulatory regions of genes, the hockey-stick plot demonstrated increased super enhancer activity upstream of UNC5B-AS1 under normoxic conditions (Fig.1C). Similarly, there was significantly increased abundance of H3K27ac modification upstream of the gene in normoxic conditions (Fig.1D). We further validated the significant downregulation of UNC5B-AS1 under hypoxic conditions in PSMCs (Fig.1E), and in response to JQ1 (an effective BET bromodomain inhibitor) treatment, the expression of UNC5B-AS1 was significantly inhibited after the chromatin

interaction was suppressed (Fig.1F). Fluorescence in situ hybridization (FISH) indicated cytoplasmic localization of UNC5B-AS1 in PSMCs (Fig.1G). Taken together, these findings suggest that UNC5B-AS1 is regulated by super enhancers in PSMCs and that its expression is downregulated and localized in the cytoplasm under hypoxic conditions.

### **FOXP3 regulates the expression of UNC5B-AS1 through chromatin remodeling.**

UNC5B-AS1, which is a super enhancer-regulated lncRNA that is downregulated under hypoxic conditions, motivated us to further investigate the upstream regulatory mechanisms driving its expression. We used three bioinformatics tools to screen for potential transcription factors that could regulate UNC5B-AS1 expression (Fig.S1A left). Based on the number and binding agent of the binding sites within the upstream promoter region of UNC5B-AS1, we identified FOXP3 as a key transcription factor that regulates UNC5B-AS1 expression (Fig.S1A right). Immunoblotting showed that FOXP3 was downregulated under hypoxic conditions (Fig.2A). Subsequently, based on the H3K27ac ChIP-seq results, we divided the upstream super enhancer region of UNC5B-AS1 into three segments (E1-E3, Fig.2B). ChIP-qPCR experiments using H3K27ac (Histone 3 Lysine 27 Acetylation, super-enhancer marker), H3K4me1 (Histone 3 Lysine 4 Monomethylation, enhancer marker), and FOXP3 antibodies revealed that FOXP3 had a strong binding affinity to segment E2 of the UNC5B-AS1 upstream super enhancer region (Fig.2C). Moreover, we divided the average span of the UNC5B-AS1 upstream promoter region into three segments (P1-P3, Fig.S1B) and performed ChIP-qPCR experiments by using H3K27ac, H3K4me1, and FOXP3 antibodies. The results demonstrated that FOXP3 has a strong binding affinity to segment P1 of the UNC5B-AS1 upstream promoter region (Fig.2D). Coimmunoprecipitation confirmed the interaction among FOXP3, H3K27ac,

and H3K4me1 (Fig.2E). These findings confirmed that FOXP3 was recruited by the upstream super enhancer E2 region and acted on the promoter P1 region of UNC5B-AS1, forming a chromatin loop to regulate the expression of the super enhancer-driven lncRNA UNC5B-AS1.

# **UNC5B-AS1 inhibits hypoxia-induced inflammatory phenotypic transition in PSMCs.**

To investigate the role of UNC5B-AS1 in hypoxic PH, we constructed an overexpression plasmid for UNC5B-AS1 and validated its overexpression efficiency by RT-qPCR (Fig.S2A). Subsequently, we overexpressed UNC5B-AS1 under hypoxic conditions and found that its overexpression significantly inhibited the transition of hypoxia-induced PSMCs from a contractile phenotype to a synthetic phenotype (Fig.3A, B and Fig.S2B). Inflammatory smooth muscle cells actively secrete inflammatory cytokines such as IL-1 $\beta$ , IL-6, and TNF- $\alpha$ <sup>29</sup>. UNC5B-AS1 overexpression notably attenuated the hypoxia-induced inflammatory phenotypic transition in PSMCs by suppressing the expression of IL-1 $\beta$ , IL-6, and TNF- $\alpha$  (Fig.3C and Fig.S2C). These results confirm that UNC5B-AS1 alleviates the hypoxia-induced inflammatory phenotypic transition in PSMCs.

# **UNC5B-AS1 inhibits PSMCs proliferation by modulating inflammatory responses.**

Smooth muscle cells (SMCs) undergo phenotypic transition toward an inflammatory phenotype and release inflammatory cytokines to participate in the perivascular inflammatory microenvironment, ultimately leading to vascular remodeling<sup>30</sup>. To investigate the crucial role of inflammatory PSMCs in the development of PH, we constructed a coculture system to simulate the inflammatory microenvironment around blood vessels. First, PSMCs were cultured under different experimental conditions for 24 hours. The cell culture supernatant (conditioned medium, CM) was collected by centrifugation, and the levels of IL-1 $\beta$ , IL-6, and

TNF- $\alpha$  were measured. A portion of the remaining conditioned medium was mixed with normal cell culture medium at a 1:1 ratio and used to stimulate normal PASMCs. Proliferation-related markers were assessed after 24 hours to evaluate the impact of the inflammatory microenvironment on normal PASMCs proliferation (Fig.S3A). Our results demonstrated that UNC5B-AS1 overexpression significantly suppressed the secretion of IL-1 $\beta$ , IL-6, and TNF- $\alpha$  in hypoxia-induced PASMCs (Fig.S3B). Conditioned media from UNC5B-AS1-overexpressing cells significantly inhibited the proliferation (Fig.S3C) of normal PASMCs under hypoxic conditions, which was accompanied by reduced cell viability (Fig.S3D) and decreased expression of PCNA (Fig.S3E). These findings suggest that UNC5B-AS1 can regulate the inflammatory microenvironment around blood vessels by suppressing the inflammatory phenotypic transition of PASMCs, thereby alleviating hypoxia-induced PASMCs proliferation.

### **UNC5B-AS1 regulates the inflammatory microenvironment in hypoxia through lactylation.**

The subcellular localization of lncRNAs determines their functions. We further examined the subcellular localization of UNC5B-AS1. By using TOMM20 as a marker of mitochondria and performing costaining with FISH, we found strong colocalization of UNC5B-AS1 with mitochondria (Fig.4A). Subsequently, we isolated cytoplasm and mitochondria, RT-qPCR showed the presence of UNC5B-AS1 in both compartments, and there was decreased expression under hypoxic conditions (Fig.4B). Mitochondria, which are central organelles involved in cellular energy metabolism, are closely related to glucose metabolism. Based on the subcellular localization of UNC5B-AS1 and abnormal glucose metabolism under hypoxic

conditions, we further assessed the impact of UNC5B-AS1 on glycolysis, as in our previous study<sup>31</sup>. Immunoblotting showed that UNC5B-AS1 overexpression inhibited the upregulation of HKII and PKM2, which are key enzymes in glycolysis during hypoxia (Fig.4C). Lactate, which is the main product of glycolysis, serves as a substrate for posttranslational modifications of proteins<sup>25</sup>. Treatment of PSMCs with the glycolysis inhibitor 2-DG attenuated the hypoxia-induced increase in protein lactylation and proliferation (Fig.S4A, B). Additionally, using panlactylation antibody, we confirmed that UNC5B-AS1 overexpression abrogated the increase in protein lactylation induced by hypoxia (Fig.4D). Finally, we assessed the H3K18la levels of the promoters of the proinflammatory cytokines IL-1 $\beta$ , IL-6, and TNF- $\alpha$ . ChIP-qPCR confirmed that UNC5B-AS1 modulated the lactylation levels of these gene promoters, thereby affecting their expression (Fig.4E). These data suggest that UNC5B-AS1 affects the lactate modification of the IL-1 $\beta$ , IL-6, and TNF- $\alpha$  promoter regions through the glycolysis pathway, thereby increasing their expression and participating in the inflammatory phenotypic transition of PSMCs.

# **UNC5B-AS1 acts as a molecular scaffold to modulate the activity of mitochondrial complex IV through LRPPRC.**

To further explore the specific mechanism by which UNC5B-AS1 influences the glycolytic pathway, we used three bioinformatics websites (catRAPID, RNAct, and RNAInter) and the subcellular localization of UNC5B-AS1 to identify LRPPRC as a downstream mitochondrial-related protein associated with UNC5B-AS1 (Fig.S5A). Immunofluorescence staining demonstrated that LRPPRC was localized within mitochondria, confirming its role as a mitochondrial-related protein (Fig.S5B). The colocalization of UNC5B-AS1 and LRPPRC

was confirmed by FISH and immunofluorescence staining (Fig.5A). Immunoblotting indicated that LRPPRC was downregulated under hypoxic conditions and that UNC5B-AS1 did not influence its expression (Fig.5B). RNA Pull-down assays (Fig.5C) and RIP experiments (Fig.5D) demonstrated the interaction between UNC5B-AS1 and LRPPRC. Based on these findings, we confirmed the interaction between UNC5B-AS1 and LRPPRC, both of which are associated with mitochondria, and the expression of LRPPRC was not affected by UNC5B-AS1.

LRPPRC was reported to exert its biological effects by influencing the activity of mitochondrial complex IV<sup>32</sup>. We propose that UNC5B-AS1 is a molecular scaffold between LRPPRC and mitochondrial complex IV, facilitating their interaction and maintaining the activity of mitochondrial complex IV. First, we designed small interfering RNAs (siRNA) targeting UNC5B-AS1 and confirmed the efficiency of UNC5B-AS1 knockdown in PSMCs (Fig.S5C). Immunoprecipitation showed that knockdown of UNC5B-AS1 affected the interaction between mitochondrial complex IV and LRPPRC (Fig.5E). Subsequently, we performed real-time monitoring of glycolysis using the Seahorse XFe24 extracellular flux analyzer. As expected, knockout of UNC5B-AS1 activated glycolysis in PSMCs under normoxic conditions, while overexpression of UNC5B-AS1 decreased glycolysis under hypoxia-induced stress (Fig.5F). Next, we evaluated the impact of UNC5B-AS1 on the activity of mitochondrial complex IV, and the results showed that knockdown of UNC5B-AS1 under normoxic conditions impaired the activity of mitochondrial complex IV, while UNC5B-AS1 overexpression alleviated the hypoxia-induced decrease in the activity of mitochondrial complex IV (Fig.5G). Finally, we assessed the effects of UNC5B-AS1 on lactate

dehydrogenase (LDH, catalyzing the conversion of pyruvate to lactate) activity and intracellular lactate levels. The results confirmed that UNC5B-AS1 overexpression inhibited the hypoxia-induced increase in LDH activity and intracellular lactate levels, while knockdown of UNC5B-AS1 under normoxic conditions increased LDH activity (Fig.5H) and intracellular lactate levels (Fig.5I). These findings confirm that UNC5B-AS1 acts as a molecular scaffold between LRPPRC and mitochondrial complex IV, thereby regulating mitochondrial metabolism and intracellular lactate production.

### **The UNC5B-AS1 conserved fragment alleviates hypoxia-induced pulmonary hypertension in vivo.**

To determine whether UNC5B-AS1 is functionally important in PH in vivo, we first used the catRAPID tool to identify the functional fragment of UNC5B-AS1 that bound to LRPPRC (Fig.S6A). We found a conserved sequence of this functional fragment in mice and named it the UNC5B-AS1 conserved fragment (UA1CF, Fig.S6B). Subsequently, we validated the expression of UA1CF in lung tissues of mice with SU5416 combined with hypoxia-induced PH (SuHx mice) by using RT-qPCR and observed the downregulation of UA1CF expression in SuHx mice (Fig.S6C). RIP experiments on mouse PSMCs confirmed the binding of UA1CF with LRPPRC (Fig.S6D). Next, we constructed an adenovirus overexpressing UA1CF and infected SuHx mice (Fig.6A). After hypoxic treatment, we assessed the impact of adenoviral infection on mice by evaluating body weight and found that there was no significant difference in body weight among the groups (Fig.S6E). RT-qPCR confirmed the successful expression of UA1CF in mouse lung tissues (Fig.6B). We then evaluated SuHx-related PH indicators in mice and found that UA1CF overexpression alleviated the increase in right



ventricular hypertrophy (Fig.6C) and right ventricular systolic pressure (RVSP, Fig.6D, E), as well as the reduction in pulmonary artery acceleration time (PAAT, Fig.6F) and pulmonary artery velocity-time integral (PAVTI, Fig.6G) in SuHx mice. However, it did not affect left heart function in mice (Fig.6H). Histological analysis (H&E staining and Masson's trichrome staining) revealed that UA1CF overexpression alleviated pulmonary arterial thickening and perivascular fibrosis in SuHx mice (Fig.6I). These results confirm that UA1CF can alleviate the symptoms of PH in SuHx mice.

### **The UNC5B-AS1 conserved fragment alleviates pulmonary inflammation in PH mice.**

Next, we evaluated the impact of UA1CF on pulmonary lactate levels and the inflammatory response in mice. UA1CF overexpression significantly alleviated the decrease in mitochondrial complex IV activity (Fig.S7A) and the increases in LDH activity and lactate levels (Fig.S7B-C) in the lung tissues of SuHx mice. Immunofluorescence staining of lung tissues showed that UA1CF overexpression alleviated pulmonary arterial lactylation (Fig.S7D) and IL-6 expression (Fig.S7E) in SuHx mice. ELISA showed that UA1CF overexpression reduced the secretion of IL-1 $\beta$ , IL-6, and TNF- $\alpha$  in the lung tissues of SuHx mice (Fig.S7F). These results indicate that UA1CF can alleviate the pulmonary inflammatory response in SuHx mice.

## **Discussion**

Previous studies have shown that UNC5B antisense lncRNA 1 (UNC5B-AS1) is involved in and functionally relevant to a spectrum of biological events. This factor regulates signaling pathways by acting as an RNA decoy and microRNA sponge<sup>33</sup>, recruiting chromatin modifiers<sup>34</sup> and inhibiting translation<sup>35</sup>. Recent studies have shown the involvement of

UNC5B-AS1 in various cancers, and it can influence the growth and metastasis of human colon cancer cells by adsorbing miR-622 and ovarian cancer progression by regulating H3K27me on NDRG2 via EZH2<sup>34</sup>. However, the role of UNC5B-AS1 in the cardiovascular or respiratory systems, particularly in the pathogenesis of pulmonary arterial hypertension, remains unknown. The present study comprehensively screened super enhancer (SE)-associated lncRNAs in PH for the first time and showed that UNC5B-AS1 was driven by SEs in PSMCs. RNA-seq data showed that UNC5B-AS1 was widely downregulated in PSMCs under hypoxic conditions, while ChIP-seq and ChIP-qPCR assays identified UNC5B-AS1 as a super enhancer transcriptional target that was directly occupied by both H3K27ac and H3K4me1. This result was further verified by the finding that JQ1 (the BET bromodomain inhibitor) dramatically suppressed the expression of UNC5B-AS1. Based on our findings, the identified landscape of SEs may provide a better mechanistic understanding of the pathophysiological role of SE-lncRNAs in PH.

SEs affect gene expression programs through the binding of transcription factors and interactions with promoters<sup>36</sup>. To examine the precise factors that regulate UNC5B-AS1 expression in response to hypoxia, we analyzed the promoter of UNC5B-AS1 and found that there were multiple binding sites for transcription factors, such as FOXP3, YY1, and USF2. We observed that FOXP3 interacted with H3K27ac and H3K4me1 to maintain chromatin looping between the UNC5B-AS1 promoter and its super enhancers and contributed to its transcriptional activity in PSMCs. Although our data indicated that UNC5B-AS1 was regulated by hypoxia in a FOXP3-dependent manner, whether other transcription factors and epigenetic regulatory factors are involved in manipulating UNC5B-AS1 expression during

hypoxic conditions in PSMCs requires further analysis.

Lactylation can occur in various cellular contexts, and is particularly under low oxygen or hypoxic conditions, catalyzed by lactate dehydrogenase enzymes<sup>37</sup>. Protein lactylation plays a crucial role in diverse biological processes, including energy metabolism<sup>38</sup>, cell signaling<sup>39</sup>, gene expression regulation<sup>40</sup>, and cell growth<sup>41</sup>. For instance, in tumor-infiltrating myeloid cells (TIMs), lactylation-driven METTL3-mediated RNA m6A modification enhances the immunosuppressive capacity of TIMs<sup>39</sup>. Furthermore, in myocardial infarction, histone lactylation regulates the dual activities of monocyte-derived macrophages by promoting the transcription of the repair genes *Lrg1*, *Vegf-α*, and *IL-10*, thereby enabling anti-inflammatory and proangiogenic responses<sup>41</sup>. Our research is the first report on the key role of lactylation in the occurrence and development of PH. The SE-lncRNA *UNC5B-AS1* plays a crucial role in maintaining the contractile phenotype of PSMCs. Under hypoxic conditions, the loss of *UNC5B-AS1* decreases the binding of LRPPRC to mitochondrial complex IV, impairing its activity and leading to aberrant activation of glycolysis, which ultimately causes intracellular lactate accumulation in PSMCs. Excessive lactate in PSMCs leads to lactylation of the upstream promoter regions of the *IL-1β*, *IL-6*, and *TNF-α* genes, thereby promoting the transition of PSMCs toward an inflammatory phenotype. This results in the release of inflammatory factors that participate in the vascular perivascular inflammatory microenvironment. By overexpressing *UNC5B-AS1* in cultured PSMCs, we further demonstrated that the hypoxia-induced inflammatory phenotype in PSMCs and the release of inflammatory factors occur in a *UNC5B-AS1*-dependent manner. These results indicate that *UNC5B-AS1* plays an important role in the development of pulmonary hypertension. Studying

the upstream lactylation sites on key genes and investigating the functions of their respective writers, readers, and erasers in PH is important.

The interaction between lncRNAs and proteins has been shown to play an important role in various biological processes. It has been reported that LRPPRC forms an RNA-dependent protein complex that is necessary for maintaining a pool of nontranslated mRNAs in mammalian mitochondria<sup>42</sup>. Studies have shown that the fibroblasts and skeletal muscle homogenates of mitochondrial disease patients showed decreased protein levels of LRPPRC and impaired complex IV enzyme activity, which were associated with abnormal complex assembly and reduced steady-state levels of numerous oxidative phosphorylation subunits<sup>43</sup>. The lncRNA SNHG17 has been shown to stabilize c-Myc protein and promote G1/S transition and cell proliferation by interacting with LRPPRC<sup>44</sup>. It can be hypothesized that LRPPRC is crucial for maintaining mitochondrial oxidative respiratory chain activity and is capable of binding to lncRNAs to exert biological effect. Our present study showed that UNC5B-AS1 could act as an LRPPRC molecular scaffold, thereby interfering with mitochondrial complex IV to modulate oxidative phosphorylation. These findings suggest that UNC5B-AS1 regulates glycolysis by modulating LRPPRC and mitochondrial complex IV. Ultimately, through lactylation, UNC5B-AS1 affects the perivascular inflammatory microenvironment and the inflammatory phenotypic transition of PSMCs, indicating that UNC5B-AS1 overexpression may provide therapeutic options for PH.

The highly conserved region of UNC5B-AS1 that binds to LRPPRC functional fragment was identified using bioinformatics tools in the mouse genome. We found that the expression of the UNC5B-AS1 conserved fragment named UA1CF was absent in the lung tissues of PH

mice induced by SU5416 combined with hypoxia (SuHx). Additionally, in mouse PSMCs, UA1CF could bind to LRPPRC. Adenovirus infection was used to overexpress UA1CF in the lungs of mice. We discovered that UA1CF could alleviate the symptoms of PH induced by SuHx in mice. Similarly, UA1CF expression in mouse lung tissues influenced the activity of mitochondrial complex IV, as well as the lactate levels and the extent of panlactylation modification in the lungs. Finally, we evaluated the levels of the inflammatory factors IL-1 $\beta$ , IL-6, and TNF- $\alpha$ , in mouse lung tissues and found that UA1CF significantly alleviated pulmonary inflammation in PH mice. Based on these results, we confirmed that UA1CF could alleviate the symptoms of PH and the levels of pulmonary inflammation in SuHx mice and provided substantial evidence supporting the beneficial role of UNC5B-AS1 in PH. Furthermore, it would be interesting to further investigate whether UA1CF was part of another novel lncRNA in the mouse genome.

In conclusion, the present study demonstrated that the SE-driven lncRNA UNC5B-AS1 plays a vital role in alleviating the inflammatory phenotype of PSMCs, thereby regulating the pathological remodeling of vessels in PH. Mechanistically, UNC5B-AS1 functioned as a novel checkpoint molecule in oxidative phosphorylation by acting as an LRPPRC molecular scaffold, thereby modulating the activity of mitochondrial complex IV. Downregulation of UNC5B-AS1 reduced the binding of LRPPRC to mitochondrial complex IV, leading to increased lactic acid levels and promoting lactylation of the promoter regions of IL-1 $\beta$ , IL-6, and TNF- $\alpha$ , thereby contributing to a perivascular inflammatory microenvironment that stimulates the proliferation of surrounding PSMCs. This finding implicates SE-lncRNAs in PH and suggests that the modulation of UNC5B-AS1 activity and its downstream targets, such as LRPPRC, is a novel

therapeutic approach for treating this hypoxia-associated disease.

## **Acknowledgments**

X.Z. designed the research, performed the experiments, analyzed the results, and wrote the manuscript. X.Z., X.W., X.G., L.Z., Z.W., X.P., J.M., L.O., Z.M., and Y.L. performed the experiments and analyzed the results. X.W., and C.M. performed and analyzed the RNA sequencing and ChIP sequencing, supervised the research, and wrote the manuscript. X.Z., and Y.C. supervised the study. F.L. and X.Z. performed the animal experiments and interpreted the results. C.M. designed and supervised the research and approved the final version of the manuscript.

## **Sources of Funding**

This work was supported by National Natural Science Foundation of China (grant numbers 82170059 and 81873412 to Cui Ma); Natural Science Foundation of Heilongjiang Province (grant number ZD2023H003 to Cui Ma); Postgraduate Research and Practice Innovation Project of Harbin Medical University (grant number YJSCX2023-99HYD to Xiangrui Zhu).

## **Disclosures**

None.

## **Supplemental Material**

Supplemental Methods

Tables S1-S4

Figure S1-S7

# References

1. Morrell NW, Adnot S, Archer SL, Dupuis J, Lloyd Jones P, MacLean MR, McMurtry IF, Stenmark KR, Thistlethwaite PA, Weissmann N, et al. Cellular and molecular basis of pulmonary arterial hypertension. *J Am Coll Cardiol.* 2009;54:S20-S31. doi: 10.1016/j.jacc.2009.04.018
2. Voelkel NF, Tudor RM. Hypoxia-induced pulmonary vascular remodeling: a model for what human disease? *J Clin Invest.* 2000;106:733-738. doi: 10.1172/JCI11144
3. Fedullo PF, Auger WR, Kerr KM, Rubin LJ. Chronic thromboembolic pulmonary hypertension. *N Engl J Med.* 2001;345:1465-1472. doi: 10.1056/NEJMra010902
4. Li D, Shao NY, Moonen JR, Zhao Z, Shi M, Otsuki S, Wang L, Nguyen T, Yan E, Marciano DP, et al. ALDH1A3 Coordinates Metabolism With Gene Regulation in Pulmonary Arterial Hypertension. *Circulation.* 2021;143:2074-2090. doi: 10.1161/CIRCULATIONAHA.120.048845
5. Ruffenach G, Medzikovic L, Aryan L, Li M, Eghbali M. HNRNPA2B1: RNA-Binding Protein That Orchestrates Smooth Muscle Cell Phenotype in Pulmonary Arterial Hypertension. *Circulation.* 2022;146:1243-1258. doi: 10.1161/CIRCULATIONAHA.122.059591
6. Hecker M, Zaslona Z, Kwapiszewska G, Niess G, Zakrzewicz A, Hergenreider E, Wilhelm J, Marsh LM, Sedding D, Klepetko W, et al. Dysregulation of the IL-13 receptor system: a novel pathomechanism in pulmonary arterial hypertension. *Am J Respir Crit Care Med.* 2010;182:805-818. doi: 10.1164/rccm.200909-1367OC
7. Omura J, Satoh K, Kikuchi N, Satoh T, Kurosawa R, Nogi M, Ohtsuki T, Al-Mamun

ME, Siddique MAH, Yaoita N, et al. ADAMTS8 Promotes the Development of Pulmonary Arterial Hypertension and Right Ventricular Failure: A Possible Novel Therapeutic Target. *Circ Res.* 2019;125:884-906. doi: 10.1161/CIRCRESAHA.119.315398

8. Xiao Y, Christou H, Liu L, Visner G, Mitsialis SA, Kourembanas S, Liu H. Endothelial indoleamine 2,3-dioxygenase protects against development of pulmonary hypertension. *Am J Respir Crit Care Med.* 2013;188:482-491. doi: 10.1164/rccm.201304-0700OC

9. Chen T, Huang JB, Dai J, Zhou Q, Raj JU, Zhou G. PAI-1 is a novel component of the miR-17~92 signaling that regulates pulmonary artery smooth muscle cell phenotypes. *Am J Physiol Lung Cell Mol Physiol.* 2018;315:L149-L161. doi: 10.1152/ajplung.00137.2017

10. Parpaleix A, Amsellem V, Houssaini A, Abid S, Breau M, Marcos E, Sawaki D, Delcroix M, Quarck R, Maillard A, et al. Role of interleukin-1 receptor 1/MyD88 signalling in the development and progression of pulmonary hypertension. *Eur Respir J.* 2016;48:470-483. doi: 10.1183/13993003.01448-2015

11. Kapranov P, Cheng J, Dike S, Nix DA, Dutttagupta R, Willingham AT, Stadler PF, Hertel J, Hackermuller J, Hofacker IL, et al. RNA maps reveal new RNA classes and a possible function for pervasive transcription. *Science.* 2007;316:1484-1488. doi: 10.1126/science.1138341

12. Wang Y, Chen W, Lian J, Zhang H, Yu B, Zhang M, Wei F, Wu J, Jiang J, Jia Y, et al. The lncRNA PVT1 regulates nasopharyngeal carcinoma cell proliferation via activating the KAT2A acetyltransferase and stabilizing HIF-1alpha. *Cell Death Differ.*



- 2020;27:695-710. doi: 10.1038/s41418-019-0381-y
13. Wang Z, Chen X, Liu N, Shi Y, Liu Y, Ouyang L, Tam S, Xiao D, Liu S, Wen F, et al. A Nuclear Long Non-Coding RNA LINC00618 Accelerates Ferroptosis in a Manner Dependent upon Apoptosis. *Mol Ther.* 2021;29:263-274. doi: 10.1016/j.ymthe.2020.09.024
14. Zhang L, Li C, Su X. Emerging impact of the long noncoding RNA MIR22HG on proliferation and apoptosis in multiple human cancers. *J Exp Clin Cancer Res.* 2020;39:271. doi: 10.1186/s13046-020-01784-8
15. Ni W, Zhang Y, Zhan Z, Ye F, Liang Y, Huang J, Chen K, Chen L, Ding Y. A novel lncRNA uc.134 represses hepatocellular carcinoma progression by inhibiting CUL4A-mediated ubiquitination of LATS1. *J Hematol Oncol.* 2017;10:91. doi: 10.1186/s13045-017-0449-4
16. Yu J, Wang W, Yang J, Zhang Y, Gong X, Luo H, Cao N, Xu Z, Tian M, Yang P, et al. LncRNA PSR Regulates Vascular Remodeling Through Encoding a Novel Protein Arteridin. *Circ Res.* 2022;131:768-787. doi: 10.1161/CIRCRESAHA.122.321080
17. Tan YT, Lin JF, Li T, Li JJ, Xu RH, Ju HQ. LncRNA-mediated posttranslational modifications and reprogramming of energy metabolism in cancer. *Cancer Commun (Lond).* 2021;41:109-120. doi: 10.1002/cac2.12108
18. Huang D, Chen J, Yang L, Ouyang Q, Li J, Lao L, Zhao J, Liu J, Lu Y, Xing Y, et al. NKILA lncRNA promotes tumor immune evasion by sensitizing T cells to activation-induced cell death. *Nat Immunol.* 2018;19:1112-1125. doi: 10.1038/s41590-018-0207-y

19. Whyte WA, Orlando DA, Hnisz D, Abraham BJ, Lin CY, Kagey MH, Rahl PB, Lee TI, Young RA. Master transcription factors and mediator establish super-enhancers at key cell identity genes. *Cell*. 2013;153:307-319. doi: 10.1016/j.cell.2013.03.035
20. Bian E, Chen X, Cheng L, Cheng M, Chen Z, Yue X, Zhang Z, Chen J, Sun L, Huang K, et al. Super-enhancer-associated TMEM44-AS1 aggravated glioma progression by forming a positive feedback loop with Myc. *J Exp Clin Cancer Res*. 2021;40:337. doi: 10.1186/s13046-021-02129-9
21. Zhang H, Xu R, Li B, Xin Z, Ling Z, Zhu W, Li X, Zhang P, Fu Y, Chen J, et al. LncRNA NEAT1 controls the lineage fates of BMSCs during skeletal aging by impairing mitochondrial function and pluripotency maintenance. *Cell Death Differ*. 2022;29:351-365. doi: 10.1038/s41418-021-00858-0
22. Dong K, Shen J, He X, Hu G, Wang L, Osman I, Bunting KM, Dixon-Melvin R, Zheng Z, Xin H, et al. CARMN Is an Evolutionarily Conserved Smooth Muscle Cell-Specific LncRNA That Maintains Contractile Phenotype by Binding Myocardin. *Circulation*. 2021;144:1856-1875. doi: 10.1161/CIRCULATIONAHA.121.055949
23. Zhang D, Tang Z, Huang H, Zhou G, Cui C, Weng Y, Liu W, Kim S, Lee S, Perez-Neut M, et al. Metabolic regulation of gene expression by histone lactylation. *Nature*. 2019;574:575-580. doi: 10.1038/s41586-019-1678-1
24. Ivashkiv LB. The hypoxia-lactate axis tempers inflammation. *Nat Rev Immunol*. 2020;20:85-86. doi: 10.1038/s41577-019-0259-8
25. Pan RY, He L, Zhang J, Liu X, Liao Y, Gao J, Liao Y, Yan Y, Li Q, Zhou X, et al. Positive feedback regulation of microglial glucose metabolism by histone H4 lysine 12

- lactylation in Alzheimer's disease. *Cell Metab.* 2022;34:634-648 e636. doi: 10.1016/j.cmet.2022.02.013
26. Irizarry-Caro RA, McDaniel MM, Overcast GR, Jain VG, Troutman TD, Pasare C. TLR signaling adapter BCAP regulates inflammatory to reparatory macrophage transition by promoting histone lactylation. *Proc Natl Acad Sci U S A.* 2020;117:30628-30638. doi: 10.1073/pnas.2009778117
27. Ma C, Li Y, Ma J, Liu Y, Li Q, Niu S, Shen Z, Zhang L, Pan Z, Zhu D. Key role of 15-lipoxygenase/15-hydroxyeicosatetraenoic acid in pulmonary vascular remodeling and vascular angiogenesis associated with hypoxic pulmonary hypertension. *Hypertension.* 2011;58:679-688. doi: 10.1161/HYPERTENSIONAHA.111.171561
28. Ma C, Wang X, He S, Zhang L, Bai J, Qu L, Qi J, Zheng X, Zhu X, Mei J, et al. Ubiquitinated AIF is a major mediator of hypoxia-induced mitochondrial dysfunction and pulmonary artery smooth muscle cell proliferation. *Cell Biosci.* 2022;12:9. doi: 10.1186/s13578-022-00744-3
29. Wang J, Xie SA, Li N, Zhang T, Yao W, Zhao H, Pang W, Han L, Liu J, Zhou J. Matrix stiffness exacerbates the proinflammatory responses of vascular smooth muscle cell through the DDR1-DNMT1 mechanotransduction axis. *Bioact Mater.* 2022;17:406-424. doi: 10.1016/j.bioactmat.2022.01.012
30. Viswanathan G, Kirshner HF, Nazo N, Ali S, Ganapathi A, Cumming I, Zhuang Y, Choi I, Warman A, Jassal C, et al. Single-Cell Analysis Reveals Distinct Immune and Smooth Muscle Cell Populations that Contribute to Chronic Thromboembolic Pulmonary Hypertension. *Am J Respir Crit Care Med.* 2023;207:1358-1375. doi:

10.1164/rccm.202203-0441OC

31. Ma C, Wang X, Zhang L, Zhu X, Bai J, He S, Mei J, Jiang J, Guan X, Zheng X, et al. Super Enhancer-Associated Circular RNA-CircKrt4 Regulates Hypoxic Pulmonary Artery Endothelial Cell Dysfunction in Mice. *Arterioscler Thromb Vasc Biol.* 2023;43:1179-1198. doi: 10.1161/ATVBAHA.122.318842
32. Cooper MP, Qu L, Rohas LM, Lin J, Yang W, Erdjument-Bromage H, Tempst P, Spiegelman BM. Defects in energy homeostasis in Leigh syndrome French Canadian variant through PGC-1alpha/LRP130 complex. *Genes Dev.* 2006;20:2996-3009. doi: 10.1101/gad.1483906
33. Zhang Y, Li Z, Lan Z. Silencing UNC5B antisense lncRNA 1 represses growth and metastasis of human Colon cancer cells via raising miR-622. *Artif Cells Nanomed Biotechnol.* 2020;48:60-67. doi: 10.1080/21691401.2019.1699809
34. Wang H, Su H, Tan Y. UNC5B-AS1 promoted ovarian cancer progression by regulating the H3K27me on NDRG2 via EZH2. *Cell Biol Int.* 2020;44:1028-1036. doi: 10.1002/cbin.11300
35. Tan SF, Ni JX, Xiong H. LncRNA UNC5B-AS1 promotes malignant progression of prostate cancer by competitive binding to caspase-9. *Eur Rev Med Pharmacol Sci.* 2020;24:2271-2280. doi: 10.26355/eurrev\_202003\_20493
36. Bal E, Kumar R, Hadigol M, Holmes AB, Hilton LK, Loh JW, Dreval K, Wong JCH, Vlasevska S, Corinaldesi C, et al. Super-enhancer hypermutation alters oncogene expression in B cell lymphoma. *Nature.* 2022;607:808-815. doi: 10.1038/s41586-022-04906-8

- 574 37. Li X, Yang Y, Zhang B, Lin X, Fu X, An Y, Zou Y, Wang JX, Wang Z, Yu T. Lactate  
575 metabolism in human health and disease. *Signal Transduct Target Ther.* 2022;7:305.  
576 doi: 10.1038/s41392-022-01151-3
- 577 38. Liberti MV, Locasale JW. Histone Lactylation: A New Role for Glucose Metabolism.  
578 *Trends Biochem Sci.* 2020;45:179-182. doi: 10.1016/j.tibs.2019.12.004
- 579 39. Xiong J, He J, Zhu J, Pan J, Liao W, Ye H, Wang H, Song Y, Du Y, Cui B, et al.  
580 Lactylation-driven METTL3-mediated RNA m(6)A modification promotes  
581 immunosuppression of tumor-infiltrating myeloid cells. *Mol Cell.* 2022;82:1660-1677  
582 e1610. doi: 10.1016/j.molcel.2022.02.033
- 583 40. Galle E, Wong CW, Ghosh A, Desgeorges T, Melrose K, Hinte LC, Castellano-Castillo  
584 D, Engl M, de Sousa JA, Ruiz-Ojeda FJ, et al. H3K18 lactylation marks tissue-specific  
585 active enhancers. *Genome Biol.* 2022;23:207. doi: 10.1186/s13059-022-02775-y
- 586 41. Wang N, Wang W, Wang X, Mang G, Chen J, Yan X, Tong Z, Yang Q, Wang M, Chen  
587 L, et al. Histone Lactylation Boosts Reparative Gene Activation Post-Myocardial  
588 Infarction. *Circ Res.* 2022;131:893-908. doi: 10.1161/CIRCRESAHA.122.320488
- 589 42. Mili S, Pinol-Roma S. LRP130, a pentatricopeptide motif protein with a noncanonical  
590 RNA-binding domain, is bound in vivo to mitochondrial and nuclear RNAs. *Mol Cell*  
591 *Biol.* 2003;23:4972-4982. doi: 10.1128/MCB.23.14.4972-4982.2003
- 592 43. Olahova M, Hardy SA, Hall J, Yarham JW, Haack TB, Wilson WC, Alston CL, He L,  
593 Aznauryan E, Brown RM, et al. LRPPRC mutations cause early-onset multisystem  
594 mitochondrial disease outside of the French-Canadian population. *Brain.*  
595 2015;138:3503-3519. doi: 10.1093/brain/awv291

44. Liu JY, Chen YJ, Feng HH, Chen ZL, Wang YL, Yang JE, Zhuang SM. LncRNA SNHG17 interacts with LRPPRC to stabilize c-Myc protein and promote G1/S transition and cell proliferation. *Cell Death Dis.* 2021;12:970. doi: 10.1038/s41419-021-04238-x

# **Highlights:**

The long non-coding RNA UNC5B-AS1, regulated by super-enhancers (SE), is downregulated in hypoxic PSMCs, and regulates PSMC phenotype transition through glycolysis.

The super-enhancer region of lncRNA UNC5B-AS1 recruits the transcription factor FOXP3 to its promoter region, forming a chromatin loop to regulate its expression.

The lncRNA UNC5B-AS1 acts as a molecular scaffold stabilizing the interaction between LRPPRC and mitochondrial complex IV.

The lactate generated by glycolysis activation induces lactylation modification of histones at the IL-1 $\beta$ , IL-6, and TNF- $\alpha$  promoters, leading to the inflammatory phenotype transition of PSMCs.

Overexpression of lncRNA UNC5B-AS1 conserved fragment reversed SuHx-induced PH in mice.

# Figures with Figure Legends

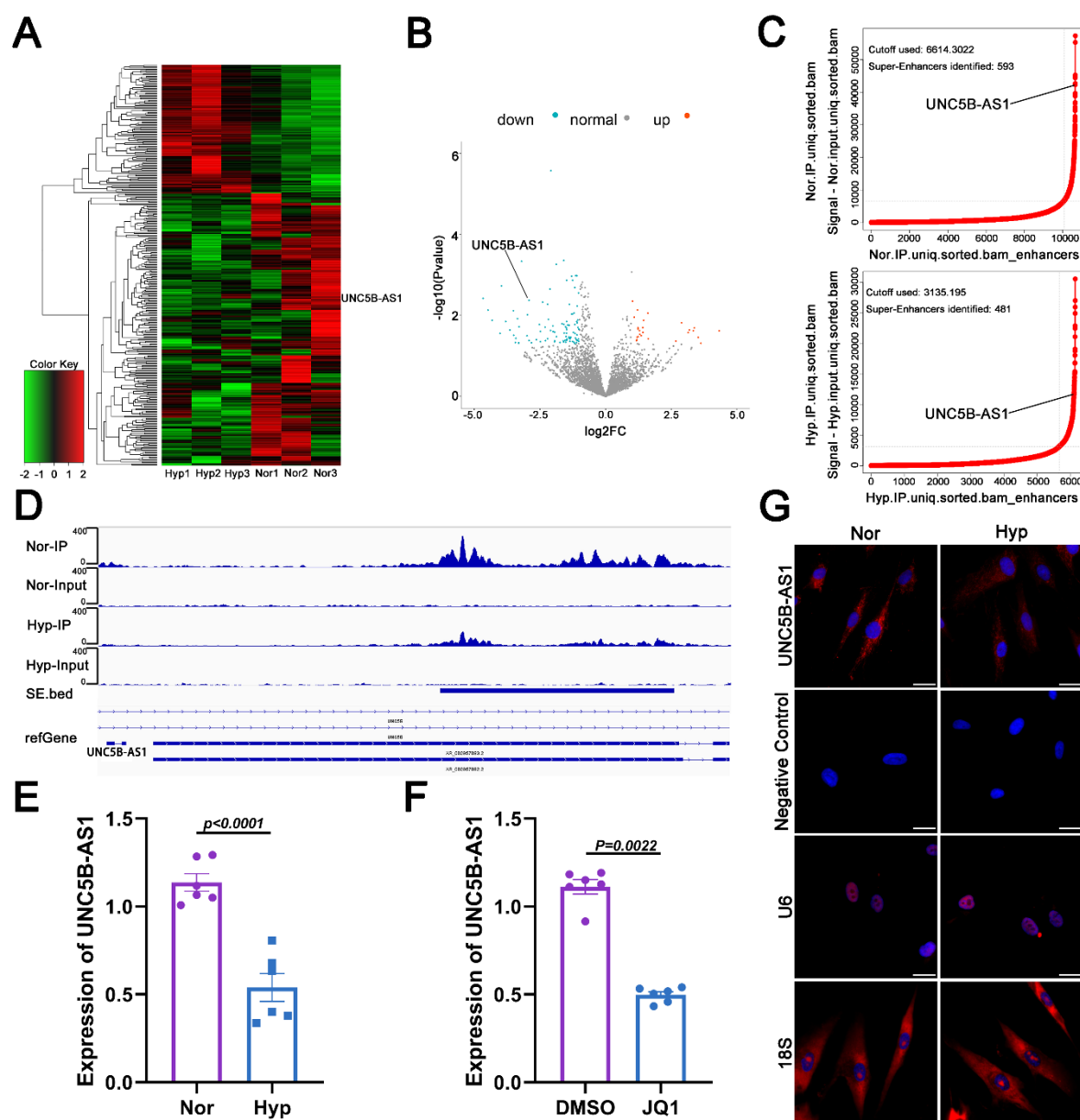


**Fig.1 The super enhancer-driven lncRNA UNC5B-AS1 is downregulated in hypoxic PASCs.**

**A** The heatmap displays the differentially expressed genes identified in normoxic/hypoxic PASCs based on RNA-seq analysis (n=3). **B** The RNA-seq results are visualized as a volcano plot, displaying the expression pattern of UNC-5B-AS1 in normoxic/hypoxic PASCs. **C** The hockey stick plot displays the activity of super enhancers and enhancers upstream of UNC5B-

AS1 in normoxic/hypoxic PSMCs (Super enhancers are defined as slope >1, while enhancers slope <1). **D** To visualize the enrichment profile of H3K27ac signal peaks upstream of UNC5B-AS1 in normoxic/hypoxic PSMCs by using IGV (Integrative Genomics Viewer). **E** The expression levels of UNC5B-AS1 in normoxic/hypoxic PSMCs (n=6). **F** The expression levels of UNC5B-AS1 after treatment of PSMCs with JQ1 (n=6). Statistical comparison was performed by the paired Student's t test (two-sided). **G** FISH results for the localization of UNC5B-AS1 in normoxic/hypoxic PSMCs. Scale bars=50μm. All data are presented as mean ± SEM. Nor, normoxia and Hyp, hypoxia.



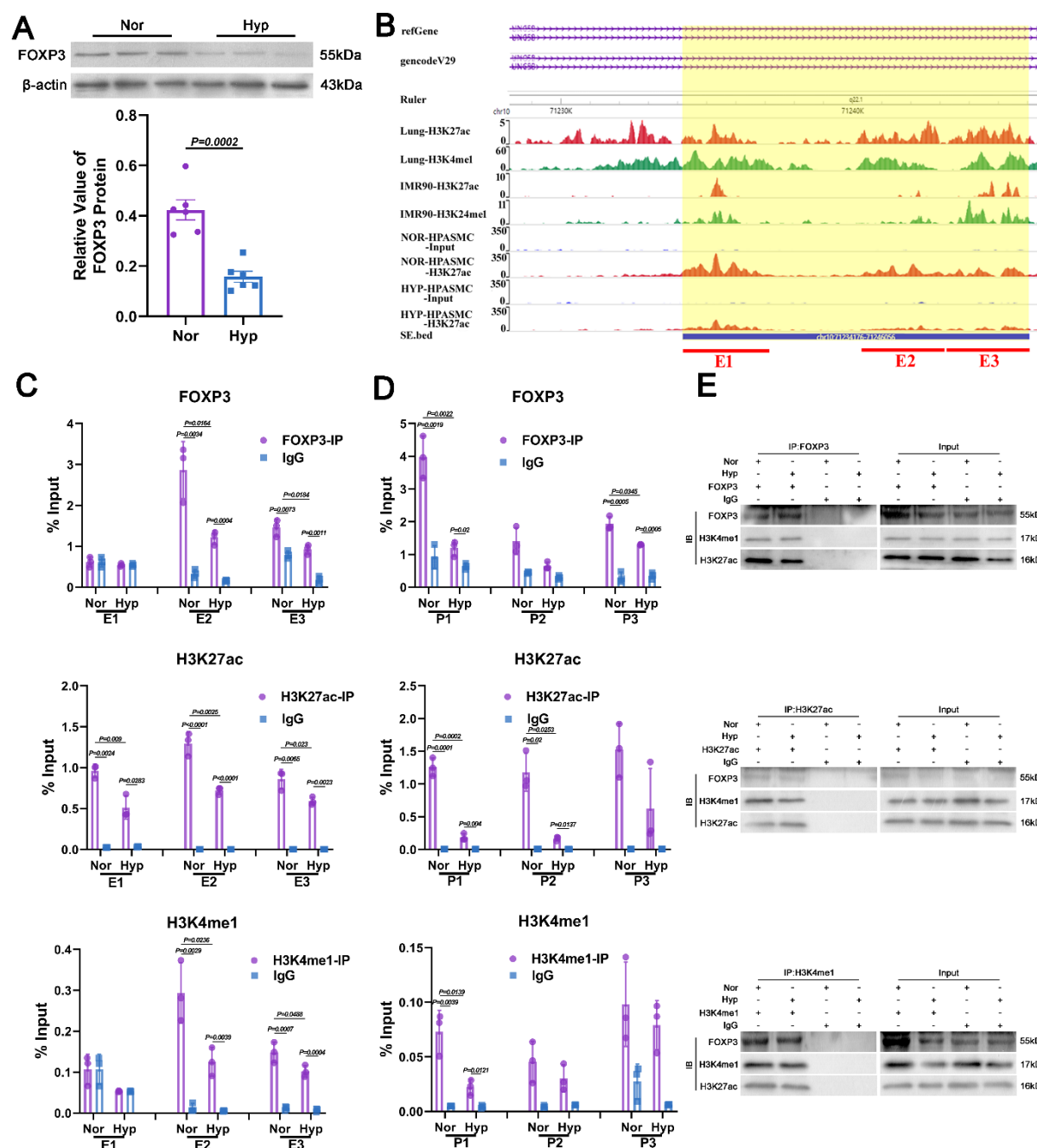


**Fig.2 FOXP3 regulates the expression of UNC5B-AS1 through chromatin remodeling.**

**A** Western blot analysis of FOXP3 in normoxic/hypoxic PASCs (n=6 ). **B** Schematic diagram illustrating the segmentation of the upstream super enhancer region of UNC5B-AS1 based on H3K27ac ChIP-seq results. FOXP3, H3K27ac, and H3K4me1 ChIP-qPCR results showing their enrichment in the upstream super enhancer region (**C**) and promoter region (**D**) of UNC5B-AS1 (n=3). **E** Results of co-immunoprecipitation with FOXP3, H3K27ac, and

637 H3K4me1. Statistical comparison was performed by the paired Student's t test (two-sided). All  
 638 data are presented as mean  $\pm$  SEM. Nor, normoxia, Hyp, hypoxia, P, promoter, E, super  
 639 enhancer, IP, immunoprecipitation, IB, Immunoblotting and IgG, Immunoglobulin G.  
 640

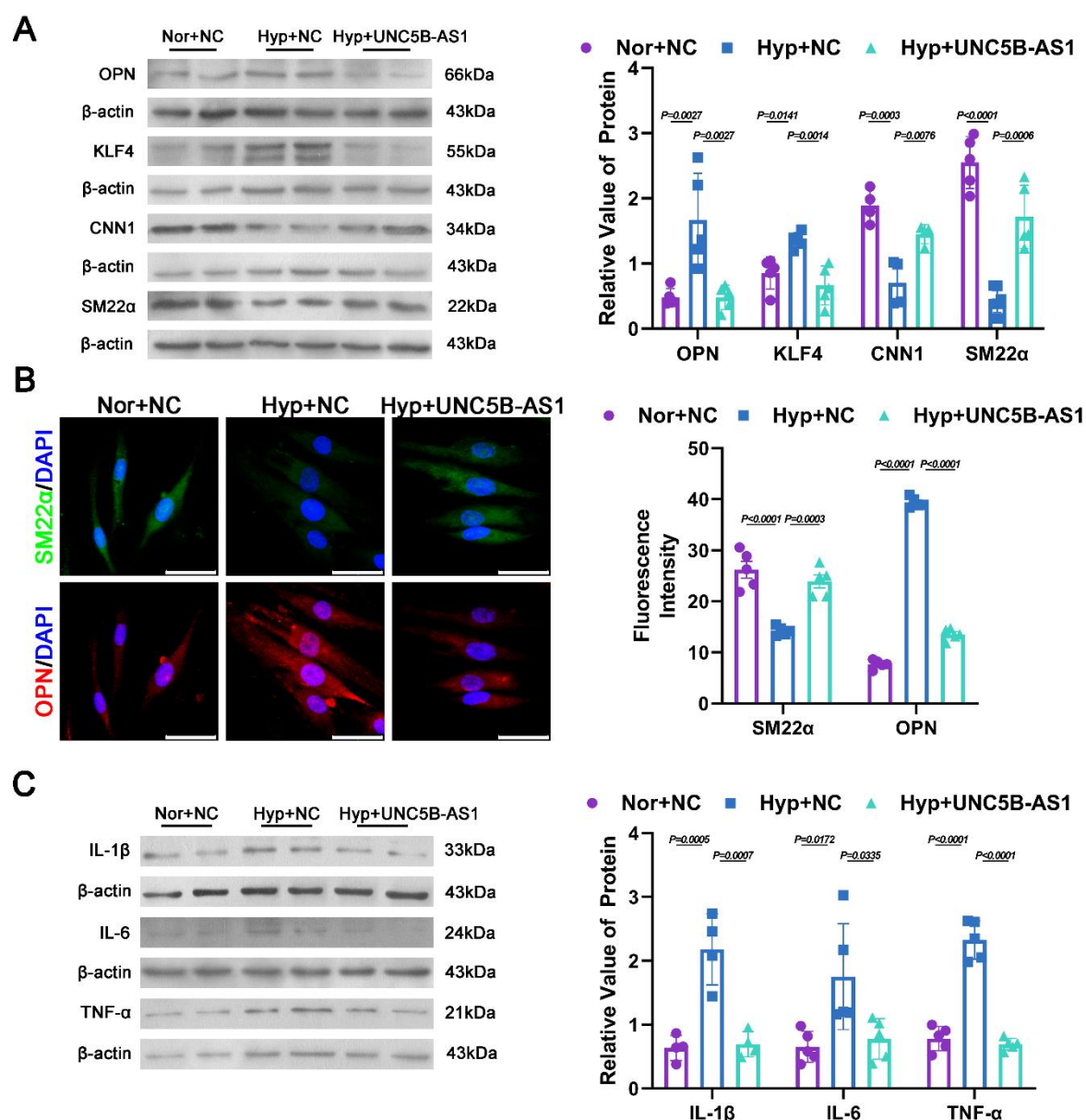


**Fig.3 UNC5B-AS1 alleviates hypoxia-induced inflammatory phenotypic transition in PSMCs.**

**A** Western blot analysis of OPN, KLF4, CNN1 and SM22α in PSMCs (n=5 for OPN, KLF4 and SM22α, n=4 for CNN1). **B** Representative immunofluorescence images of PSMCs stained with anti-SM22α (green) antibody, anti-OPN (red) antibody and DAPI (blue). Scale bars=100 μm. **C** Western blot analysis of IL-1β, IL-6 and TNF-α in PSMCs (n=5 for IL-6 and TNF-α, n=4 for IL-1β). All data are presented as mean ± SEM. One-way ANOVA with Tukey

649 post hoc test was used to compare multiple groups with equal variance, and Brown-Forsythe  
650 and Welch ANOVA with Tamhane T2 post hoc test was used to compare multiple groups with  
651 unequal variance. Nor, normoxia, Hyp, hypoxia, NC, Negative control and UNC5B-AS1,  
652 UNC5B-AS1 overexpression.  
653

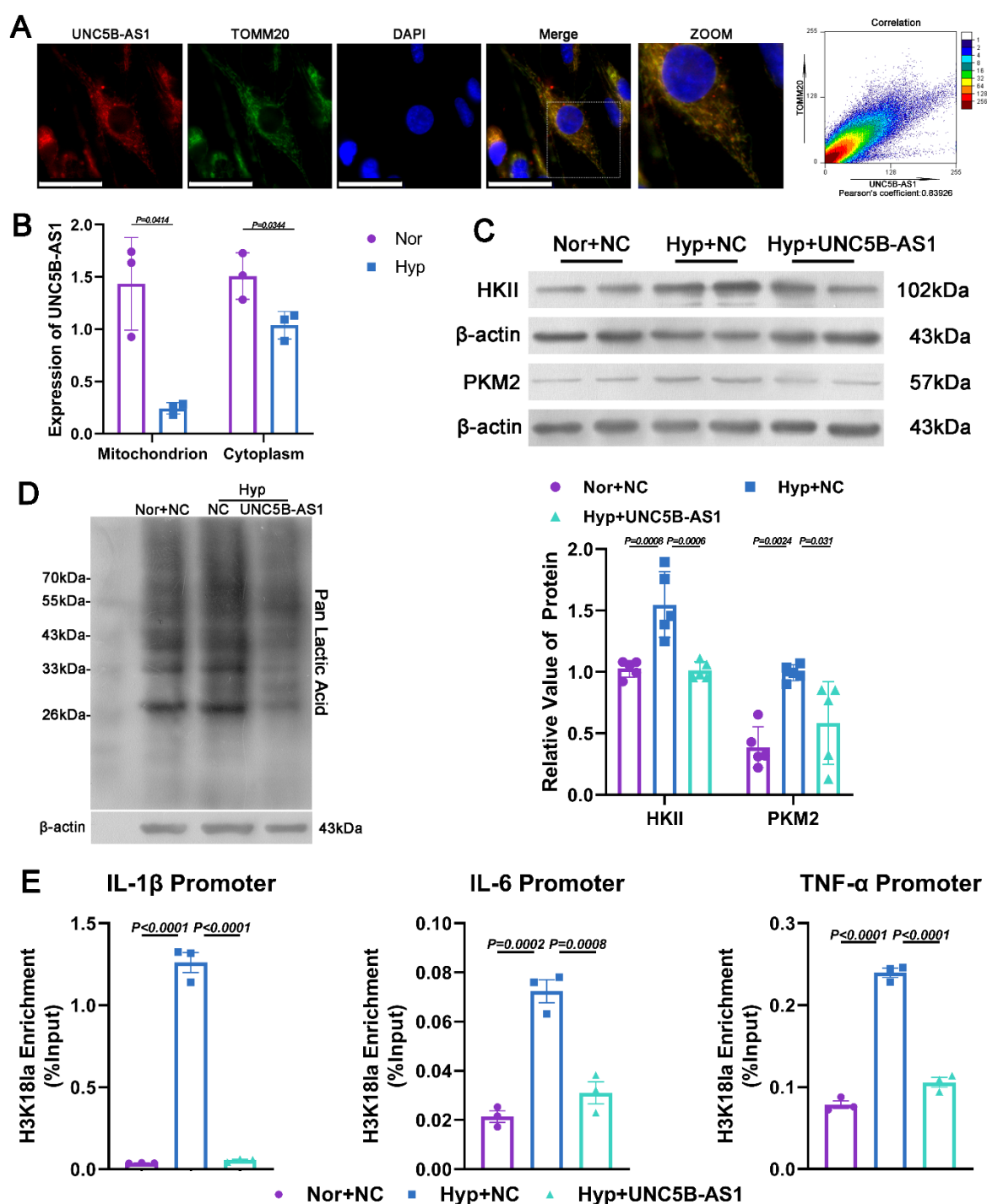


**Fig.4 UNC5B-AS1 inhibits the expression of inflammatory factors through lactylation modification.**

**A** Representative immunofluorescence images of PSMCs stained with anti-TOMM20 (green) antibody, UNC5B-AS1 probe (red) and DAPI (blue), the Pearson correlation coefficient reflects the correlation between two fluorescence labels in co-localization. Scale bars=100 μm.

**B** Expression of UNC5B-AS1 in PASMCMitochondrion and cytoplasm (n=3). Statistical comparison was performed by the paired Student's t test (two-sided). **C** Western blot analysis of the expression of HKII and PKM2 in PASMCMs (n=5). **D** Western blot analysis of pan-lactylation modification in PASMCMs. **E** ChIP-qPCR analysis of H3K18la modification in IL-1 $\beta$ , IL-6 and TNF- $\alpha$  promoter (n=3). All data are presented as mean  $\pm$  SEM. One-way ANOVA with Tukey post hoc test was used to compare multiple groups with equal variance, and Brown-Forsythe and Welch ANOVA with Tamhane T2 post hoc test was used to compare multiple groups with unequal variance. Nor, normoxia, Hyp, hypoxia, NC, Negative control and UNC5B-AS1, UNC5B-AS1 overexpression.

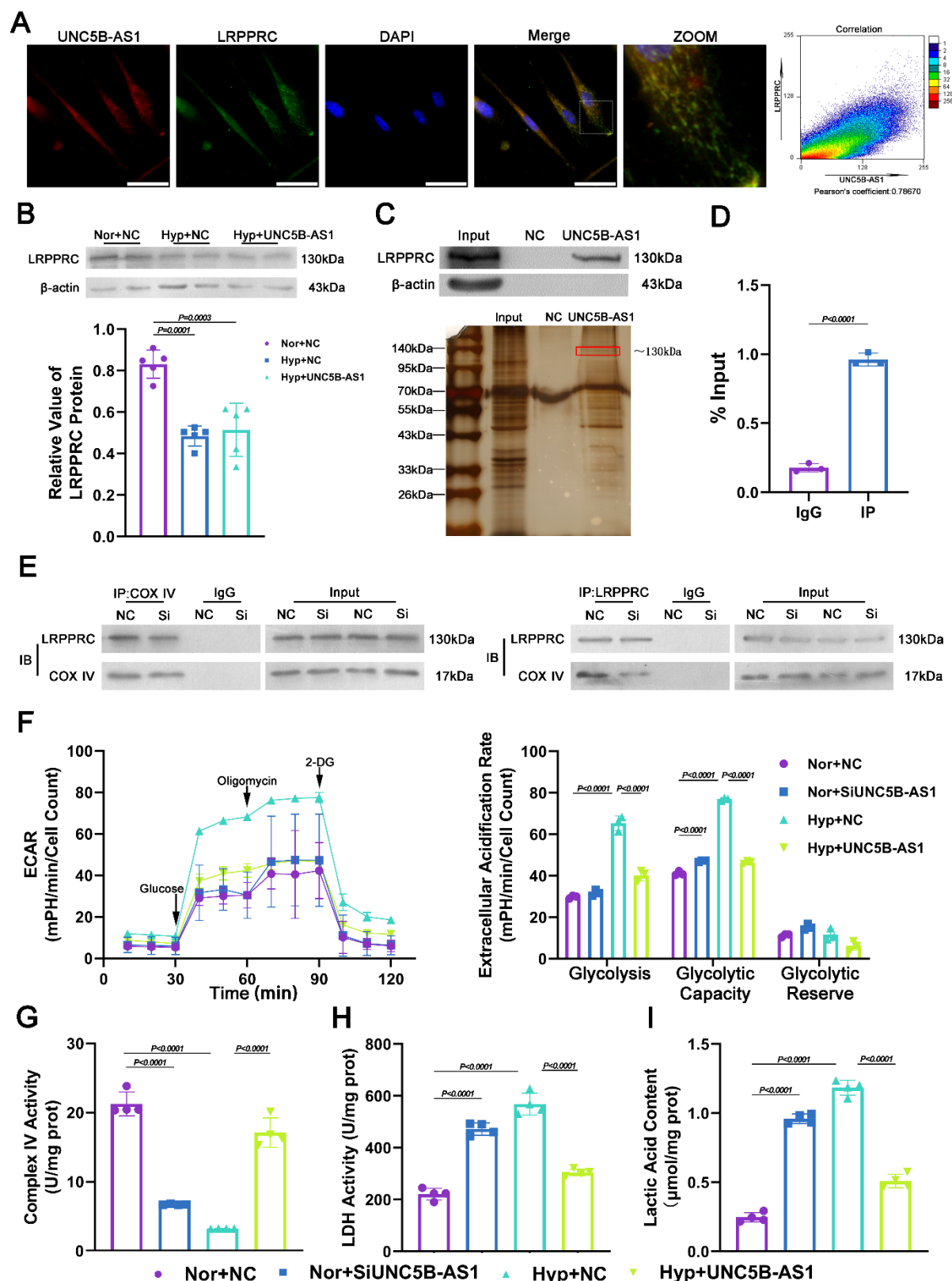


**Fig.5 UNC5B-AS1 acts as a molecular scaffold by binding to LRPPRC, influencing the activity of mitochondrial complex IV.**

**A** Representative immunofluorescence images of PSMCs stained with anti-LRPPRC (green) antibody, UNC5B-AS1 probe (red) and DAPI (blue), the Pearson correlation coefficient reflects the correlation between two fluorescence labels in co-localization. Scale bars=100  $\mu$ m.

**B** Western blot analysis of LRPPRC in PSMCs (n=5). **C** Up panel, RNA pull-down analysis was performed to examine the binding between UNC5B-AS1 and LRPPRC in PSMCs. Below panel, silver staining results of RNA Pull-down in PSMCs. **D** RIP analysis was performed to examine the binding between UNC5B-AS1 and LRPPRC in PSMCs (n=3). Statistical comparison was performed by the paired Student's t test (two-sided). **E** Results of co-immunoprecipitation with mitochondrial complex IV (COX IV) and LRPPRC after siUNC5B-AS1. **F** Glycolysis and glycolytic reserve following treatment with 10 mmol/L glucose and 1  $\mu$ M oligomycin were measured in cultured PSMCs, and nonglycolytic acidification after treatment with 100 mmol/L 2-deoxyglucose was detected (n=3). Mitochondrial complex IV activity (**G**), LDH activity (**H**) and intracellular lactic acid contents (**I**) in PSMCs (n=4). All data are presented as mean  $\pm$  SEM. One-way ANOVA with Tukey post hoc test was used to compare multiple groups with equal variance, and Brown-Forsythe and Welch ANOVA with Tamhane T2 post hoc test was used to compare multiple groups with unequal variance. Nor, normoxia, Hyp, hypoxia, NC, Negative control, SiUNC5B-AS1, UNC5B-AS1 small interfering RNA and UNC5B-AS1, UNC5B-AS1 overexpression.



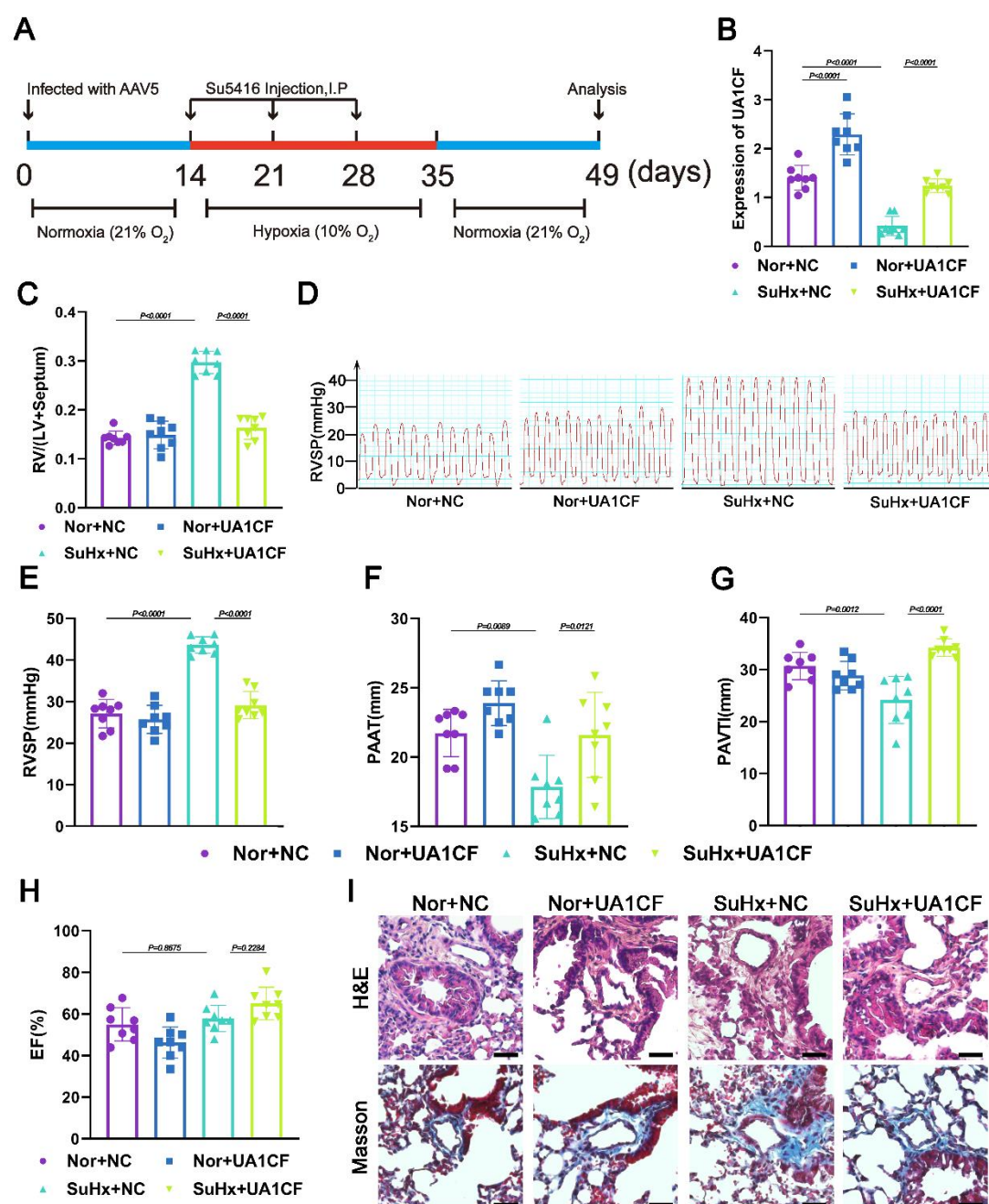


**Fig. 6 UNC5B-AS1 conserved fragment alleviates SuHx-induced PH in mice.**

**A** Schematic diagram of the SU5416 combined with hypoxia-induced PH (SuHx) mice model.

**B** Expression of UNC5B-AS1 conserved fragment (UA1CF) in mice lungs (n=8). **C** Right

ventricle/left ventricle + septum (RV/LV+ Septum) in mice (n=8). **D** Representative waveform

of right ventricular systolic pressure. **E** Representative right ventricular systolic pressure

(RVSP) in mice (n=8). Pulmonary artery acceleration time (PAAT, **F**), pulmonary artery

697 velocity-time integral (PAVTI, **G**), ejection fraction (EF, **H**) in mice (n=8). **I** Representative  
698 images of Hematoxylin and Eosin staining (H&E) and Masson staining in mice lungs. Scale  
699 bars=50  $\mu$ m. All data are presented as mean  $\pm$  SEM. One-way ANOVA with Tukey post hoc  
700 test was used to compare multiple groups with equal variance, and Brown-Forsythe and Welch  
701 ANOVA with Tamhane T2 post hoc test was used to compare multiple groups with unequal  
702 variance. Nor, normoxia, SuHx, SU5416 combined with hypoxia, NC, Negative control and  
703 UA1CF, AAV5-UNC5B-AS1 conserved fragment overexpression.